Performance evaluation of decentralized wireless sensing and control in civil structures

Yang Wang [*a], R. Andrew Swartz [b], Jerome P. Lynch [b], Kincho H. Law [a], Chin-Hsiung Loh [c]
[a] Dept. of Civil and Environmental Engineering, Stanford Univ., Stanford, CA 94305
[b] Dept. of Civil and Environmental Engineering, Univ. of Michigan, Ann Arbor, MI 49109
[c] Dept. of Civil Engineering, National Taiwan Univ., Taipei, Taiwan, 106 R.O.C.

ABSTRACT

A structural control system consists of sensors, controllers, and actuators integrated in a single network to effectively mitigate building vibration during external excitations. The costs associated with high-capacity actuators and system installation are factors impeding the wide spread adoption of structural control technology. Wireless communication can potentially lower installation costs by eliminating coaxial cables and offer better flexibility and adaptability in the design of a structural control system. This paper introduces a prototype wireless sensing and control unit that can be incorporated in a real-time structural control system. Tests are conducted using a 3-story half-scale laboratory structure instrumented with magnetorheological dampers to validate the feasibility of the wireless structural control system. This paper also addresses the serious issue of time delay and communication range inherent to wireless technologies. Numerical simulations using different decentralized structural control strategies are conducted on a 20-story steel structure controlled by semi-active hydraulic dampers.

Keywords: structural control, wireless communication, embedded computing, decentralized output feedback control.

1. INTRODUCTION

For the past three decades, significant advances have been made in structural control [1]. Hardware technologies and control theories are now widely available for exploration in civil structural applications. It is reported that between 1989 and 2003, about 50 buildings and towers have been instrumented with various types of structural control systems with evident reduction in structural dynamic responses being observed [2].

Structural control systems can be categorized into three major types: (a) passive control (e.g. base isolation), (b) active control (e.g. active mass dampers), and (c) semi-active control (e.g. semi-active variable dampers). Passive control systems utilize passive energy dissipation devices to mitigate structural vibration. These types of control systems require minimum amount of operational power and complexity, but they lack adaptability to real-time external excitations. On the other hand, active control systems are adaptable to external excitations by adjusting actuation forces through a real-time feedback control loop, but the active control devices are usually power hungry. The operation of these active control devices often depends on power lines in the building, which may not be reliable during extreme natural events. Semi-active control effectively combines the merits of active and passive control techniques. Semi-active control devices are power-efficient and their actuation forces are adjustable through feedback control. Examples of semi-active actuators include active variable stiffness (AVS) devices, semi-active hydraulic dampers (SHD), electrorheological (ER) dampers, and magnetorheological (MR) dampers. Similar to passive control systems, semi-active control systems are inherently stable because their actuators do not apply mechanical energy directly to the structure. To facilitate feedback control in a semi-active control system, structural sensors are employed to measure the dynamic response of a structure in real-time. Sensor data are fed into control modules to compute optimal actuation forces. The actuation forces are then applied to the structure through semi-active control devices to mitigate excessive dynamic responses.

In traditional semi-active control systems, coaxial cables are installed to connect sensors, controllers, and actuators for feedback control. As the size of the structure increases, the cost of installing the wires also grows. Furthermore, once a cabled control system is installed, reconfiguring the system would require costly rerouting of the cables. To eliminate

[*] wyang98@stanford.edu; phone 1 650 723-6213; fax 1 650 725-9755; http://eil.stanford.edu/wimms

the cost and inconvenience of cable installation, wireless communication and embedded computing technologies can be viable alternatives in structural control applications. Wireless communication has been extensively explored for use in structural health monitoring [3-4]. However, only a few studies have been reported on incorporating wireless communication in real-time feedback structural control [5-6]. In these studies, sensor data is transmitted wirelessly to wireless control units where embedded control algorithms determine control actions to be applied to actuators.

One important issue about real-time feedback structural control is the latencies for transmitting sensor data and control commands wirelessly. In order to achieve good performance, the communication latency should be kept as low as possible. In centralized control, regardless of wired or wireless communication, the control server has to collect data from all the sensors in the structure. The communication latency increases with the size of the structure and the number of sensors being deployed. Moreover, the centralized control server represents a single-point of failure of the entire control system. To alleviate these issues, decentralized control strategies can be explored [7]. In decentralized control architectures, sensors and controllers are distributively placed in a structure. Each controller collects data from the nearby sensors and executes commands on the nearby structural actuators. Therefore, the communication ranges are significantly shorter and the communication latency decreases since the number of sensors or actuators that each controller has to communicate with is significantly smaller. Decentralization also allows large quantities of lower-capacity actuators to be deployed in the structure, which could be much cheaper to fabricate than actuators with very high force capacities. As the control decisions are computed and executed distributively by individual controllers, system redundancy and reliability can also be improved.

This study investigates the feasibility and issues in wireless sensing and decentralized control. A prototype hardware and software system is developed for wireless structural sensing and control with both centralized and decentralized control strategies embedded in the system. Validation of the wireless sensing and control system was conducted on a half-scale three-story steel structure instrumented with magnetorheological (MR) dampers. The experiments show that by reducing communication latency, decentralized control strategies can achieve reliable control performance comparable to their centralized counterparts. To further investigate the feasibility of decentralized structural control on large-scale structures, numerical simulations of a 20-story steel-frame structure have been carried out. Preliminary results from these numerical simulations illustrate the effectiveness of decentralized structural control strategies.

2. EXPERIMENTS ON DECENTRALIZED WIRELESS STRUCTURAL CONTROL

In this section, a prototype wireless structural sensing and control system is first introduced. Centralized and decentralized structural control algorithms with time-delayed output feedbacks are then described. This section also presents the experimental setup and results for the validation tests of the wireless prototype system on a half-scale three-story steel structure instrumented with magnetorheological (MR) dampers.

2.1 A prototype wireless structural sensing and control system

Fig. 1 illustrates a 3-story structure instrumented with the prototype wireless sensing and control system. The system consists of wireless sensors and controllers that are mounted on the structure for measuring structural response data and commanding actuators in real-time. Besides the wireless sensing and control units that are necessary for data collection and the operation of the actuators, a remote command server with a wireless transceiver is included in the system for experimental purpose. In a laboratory experiment, the server is designed to initiate the operation of the control system and to log the flow of wireless data. To initiate the operation, the command server first broadcasts a start signal to all of the wireless sensing and control units. Once the start command is received, the wireless units that are responsible for collecting sensor data start acquiring and broadcasting data at a preset time interval. Accordingly, the wireless units responsible for commanding the actuators receive the sensor data, calculate desired control forces, and apply control commands within the specified time interval assigned at each time step.

The wireless unit is designed in such a way that each unit can serve as either a sensing unit, or a control unit, or a unit for both sensing and control. This flexibility is supported by an integrated hardware design based upon a wireless sensing unit (Fig. 1b) previously proposed for wireless structural monitoring [8]. The three original functional modules included in the wireless sensing unit design are the sensor signal digitizer, the computational core, and the wireless transceiver. To extend the functionality of the wireless sensor for actuation, an off-board actuation signal generation module (Fig. 1c) is designed and fabricated. The actuation signal generation module consists of a single-channel 16-bit digital-to-analog converter and other support electronics. The module receives digital integers from a wireless sensing unit and converts the digital signal into an analog voltage ranging from -5V to 5V. This voltage signal then commands the associated

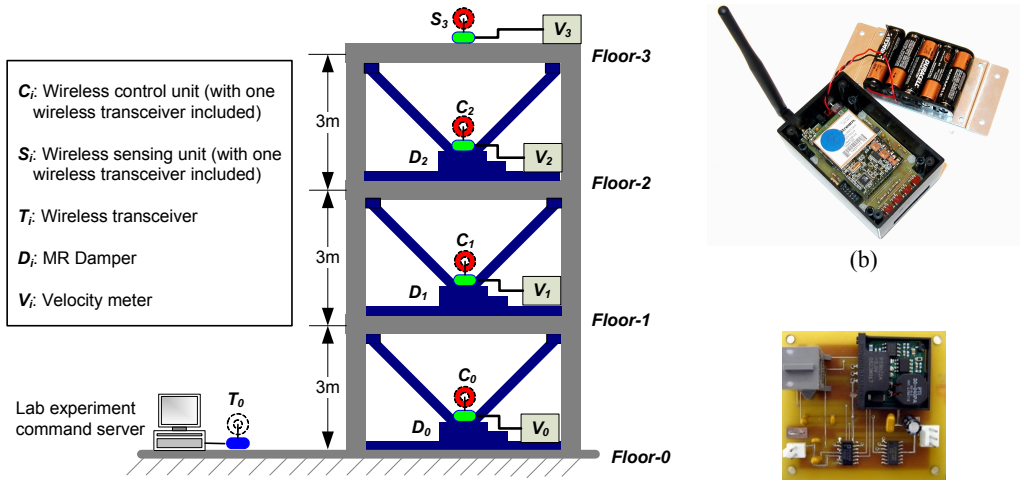

Fig. 1. Overview to the prototype wireless sensing and control system: (a) a 3-story structure controlled by three actuators; (b) packaged wireless sensing and control unit (10.2 × 6.5 × 4.0 cm^3); (c) printed circuit board of the actuation signal generation module (5.5 × 6.0 cm^2).

structural actuator that applies actuation forces to the controlled structure. Detailed design of the wireless sensing and control unit and the actuation signal generation module has been described in Ref. [5].

2.2 Centralized and decentralized control algorithms using time-delayed output feedback

In this feasibility study, an output feedback control algorithm based on linear quadratic regulation (LQR) is employed. The algorithm can be briefly summarized as follows. For a lumped-mass structural model with n degrees-of-freedom (DOF) and m actuators, the system state-space equation considering l time steps of delay can be formulated as:

$$\mathbf{z}_d[k+1] = \mathbf{A}_d \mathbf{z}_d[k] + \mathbf{B}_d \mathbf{p}_d[k-l], \text{ where } \mathbf{z}_d[k] = \begin{Bmatrix} \mathbf{x}_d[k] \\ \dot{\mathbf{x}}_d[k] \end{Bmatrix} \tag{1}$$

Here $\mathbf{z}_d[k]$ represents the $2n \times 1$ discrete-time state-space vector, $\mathbf{p}_d[k-l]$ is the delayed $m \times 1$ control force vector, $\mathbf{A}_d$ is the $2n \times 2n$ system matrix (containing the information about structural mass, stiffness, and damping), and $\mathbf{B}_d$ is the $2n \times m$ actuator location matrix. For the experiments and simulations presented in this paper, we consider the case where l is equal to 1, i.e. the time delay is equal to one sampling time step. The primary objective of the time-delay LQR problem is to minimize a cost function J by selecting an optimal control force trajectory $\mathbf{p}_d$:

$$J\big|_{\mathbf{p}_d} = \sum_{k=l}^{\infty} \left(\mathbf{z}_d^T[k] \mathbf{Q} \mathbf{z}_d[k] + \mathbf{p}_d^T[k-1] \mathbf{R} \mathbf{p}_d[k-1] \right), \text{ where } \mathbf{Q}_{2n \times 2n} \geq 0 \text{ and } \mathbf{R}_{m \times m} > 0 \tag{2}$$

In an output feedback control design, control decisions are computed based on real-time measurement data in the $q \times 1$ system output vector $\mathbf{y}_d[k]$. The output vector is defined by a $q \times 2n$ linear transformation, $\mathbf{D}_d$, to the state-space vector $\mathbf{z}_d[k]$:

$$\mathbf{y}_d[k] = \mathbf{D}_d \mathbf{z}_d[k] \tag{3}$$

For example, if the relative velocities on all floors (but not the relative displacements) are measurable, $\mathbf{D}_d$ can be defined (by letting $q = n$) as:

$$\mathbf{D}_{d1} = \begin{bmatrix} \mathbf{0}_{n \times n} & \mathbf{I}_{n \times n} \end{bmatrix} \tag{4}$$

In another example, if inter-story velocities between adjacent floors are measurable, the output matrix $\mathbf{D}_\mathbf{d}$ can be defined (by letting $q = n$) as:

$$\mathbf{D}_{\mathbf{d2}} = \left[\begin{array}{c|ccccc} & 1 & 0 & 0 & \cdots & 0 \\ & -1 & 1 & 0 & \cdots & 0 \\ \left[\mathbf{0}_{n\times n}\right] & 0 & -1 & 1 & \cdots & 0 \\ & \vdots & \ddots & \ddots & \ddots & \vdots \\ & 0 & \cdots & 0 & -1 & 1 \end{array}\right]_{n\times 2n} \tag{5}$$

The $m \times q$ optimal gain matrix $\mathbf{G}_\mathbf{d}$ is designed to provide the optimal output feedback control force:

$$\mathbf{p}_\mathbf{d}[k] = \mathbf{G}_\mathbf{d}\mathbf{y}_\mathbf{d}[k] \tag{6}$$

Chung *et al*. [9] proposed the formulation to the above output feedback control problem considering time delay (l time steps). As a result, a set of coupled nonlinear matrix equations can be solved for an optimal output feedback gain matrix $\mathbf{G}_\mathbf{d}$. In our implementation, an iterative algorithm put forth by Lunze [10] is modified to solve the matrix equations. The algorithm described by Lunze also provides the flexibility to handle additional external constraints. In particular, this algorithm can compute a suboptimal control solution for a decentralized system simply by constraining the structure of $\mathbf{G}_\mathbf{d}$ to be consistent with the decentralized architecture [11]. For example, the following equations illustrate the constrained structures of two decentralized output feedback gain matrices for a 3-story lumped-mass structure ($n = 3$):

$$\mathbf{G}_{\mathbf{d1}} = \begin{bmatrix} * & 0 & 0 \\ 0 & * & 0 \\ 0 & 0 & * \end{bmatrix}, \quad \mathbf{G}_{\mathbf{d2}} = \begin{bmatrix} * & * & 0 \\ 0 & * & * \\ 0 & * & * \end{bmatrix} \tag{7}$$

Combining with the output matrix $\mathbf{D}_\mathbf{d}$ defined in Eq. (4) or (5), the pattern in $\mathbf{G}_{\mathbf{d1}}$ specifies that when computing control decisions, the actuator at each floor only needs the entry in the output vector $\mathbf{y}_\mathbf{d}$ that corresponds to that floor. The pattern in $\mathbf{G}_{\mathbf{d2}}$ specifies that the control decisions also require information from a neighboring floor.

2.3 Validation experiments

To study the potential application of the wireless sensing and control system for decentralized structural control, validation tests on a 3-story frame structure instrumented with MR dampers are conducted at the National Center for Research on Earthquake Engineering (NCREE) in Taipei, Taiwan (Fig. 2a). The floor plan of this structure is 3m × 2m, with each floor weight adjusted to 6,000 kg using concrete blocks. The inter-story height is 3m. Both the beams and the columns of the structure are constructed with H150 × 150 × 7 × 10 steel I-beam elements. The three-story structure is mounted on a 5m × 5m 6-DOF shake table. The shake table can generate ground excitations with frequencies spanning from 0.1Hz to 50Hz. For this study, only longitudinal excitations are used. Along this direction, the shake table can excite the structure with a maximum acceleration of 9.8 m/s^2. The excitation has a maximum stroke and force of ±0.25m and 220 kN, respectively. The test structure is heavily instrumented with accelerometers, velocity meters, and linear variable displacement transducers (LVDT) installed on each floor of the structure to measure the dynamic response. These sensors are interfaced to a high-precision wire-based data acquisition (DAQ) system native to the NCREE facility; the DAQ system is set to a sampling rate of 200 Hz. A separate set of wireless sensors are installed as part of the wireless control system.

For the experimental study, three 20 kN MR dampers are installed with V-braces on each story of the steel structure (Fig. 2b). The damping coefficients of the MR dampers can be changed by issuing a command voltage between 0V to 1.2V. This command voltage determines the electric current of the electromagnetic coil in the MR damper, which in turn, generates a magnetic field that sets the viscous damping properties of the MR damper. Calibration tests were first conducted on the MR dampers before mounting them to the structure so that modified Bouc-Wen damper models can be formulated for each damper [12]. In the real-time feedback control tests, hysteresis model parameters for the MR dampers are an integral element in the calculation of damper actuation voltages. Fig. 2(c) illustrates a wireless control unit and an off-board control signal generation module that work together to command an MR damper.

(a)

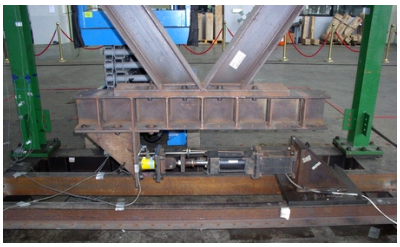

(b)

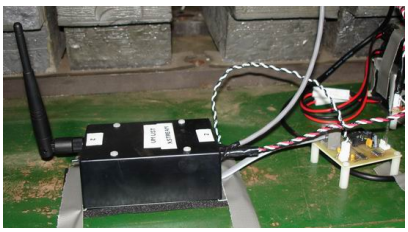

(c)

Fig. 2. Laboratory setup: (a) the 3-story test structure mounted on the shake table; (b) the MR damper installed between the 1st floor and the base floor of the structure; (c) a wireless control unit and an off-board control signal generation module.

Table 1. Different decentralization patterns and sampling times for the wireless and wire-based control experiments.

	Wireless System			**Wired System**
Degree of Centralization	1	2	3	3
Gain Matrix Pattern	$\mathbf{G}_{d1}$ in Eq. (7)	$\mathbf{G}_{d2}$ in Eq. (7)	N/A	N/A
Output Matrix	$\mathbf{D}_{d2}$ in Eq. (5)	$\mathbf{D}_{d2}$ in Eq. (5)	$\mathbf{D}_{d1}$ in Eq. (4)	$\mathbf{D}_{d1}$ in Eq. (4)
Sampling Time/Rate	0.02s / 50Hz	0.06s / 16.67Hz	0.08s / 12.5Hz	0.005s / 200Hz

For the wireless system, a total of four wireless sensors are installed, following the deployment shown in Fig. 1(a). Each wireless sensor is interfaced to a Tokyo Sokushin VSE15-D velocity meter to measure the absolute velocity response for each floor of the structure, as well as the base. The sensitivity of this velocity meter is 10V/(m/s) with a measurement limit of ±1 m/s. The three wireless sensors on the first three levels of the structure (C_0, C_1, and C_2) are also responsible for commanding the MR dampers. Besides the wireless control system, a traditional wire-based control system is installed in the structure for comparative analyses. Centralized and decentralized velocity feedback control schemes are used for the wired and the wireless control systems. Table 1 summarizes the different patterns of the gain matrix, $\mathbf{G}_d$, the output matrices, $\mathbf{D}_d$, and the achievable sampling times for the centralized, partially decentralized and fully decentralized control strategies (which are denoted by degrees of decentralization, 3, 2 and 1, respectively). For this test structure, the wire-based system can achieve a sampling rate of 200 Hz, or a time step of 0.005 s. Mostly decided by the communication latency of the 24XStream wireless transceivers, the wireless system can achieve a sample rate of 12.5 Hz (or a time step of 0.08 s) for the centralized control scheme. This sample rate is due to each wireless sensor waiting in turn to communicate its data to the network (about 0.02 s for each transmission). An advantage of the decentralized architecture is that fewer communication steps are needed, thereby reducing the time for wireless communication.

To ensure that appropriate control decisions are computed by the wireless control units, one necessary condition is that the real-time velocity data used by them are accurate. Rarely experiencing data losses during the experiments, our prototype wireless sensor network proves to be robust. In case data loss happens, the wireless control unit is currently designed to simply use a previous data sample. For the experimental results presented herein, the ground excitation is the 1940 El Centro NS earthquake record (Imperial Valley Irrigation District Station) scaled to a peak ground acceleration of 1 m/s^2. To illustrate the performance of different decentralized schemes with various communication latencies, the same ground excitation is applied to the original uncontrolled structure with four different wired and

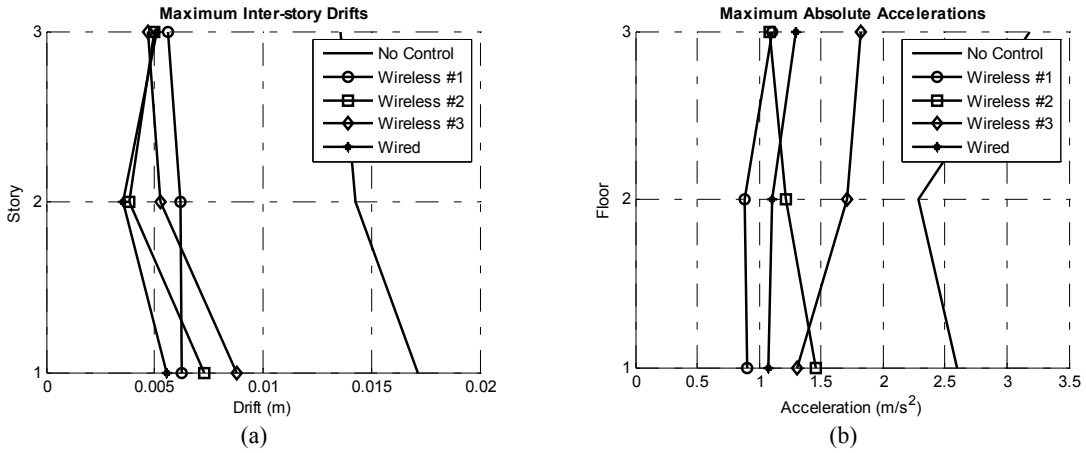

Fig. 3. Experimental results of different control schemes using the El Centro excitation scaled to a peak acceleration of 1 m/s^2: (a) peak inter-story drifts; (b) peak absolute accelerations.

wireless control schemes implemented, as defined in Table 1. Fig. 3 illustrates the structure's peak inter-story drifts and floor absolute accelerations during these experimental runs. Compared with the uncontrolled structure, all wireless and wired control schemes achieve significant reduction with respect to maximum inter-story drifts and absolute accelerations. Among the four control cases, the wired centralized control scheme shows better performance in achieving the least peak drifts and second least overall peak accelerations. This result is rather expected, because the wired system has the advantages of lower communication latency and utilizes complete sensor data from all floors. The wireless schemes, although running at longer sampling steps, achieve control performance comparable to the wired system. The fully decentralized wireless control scheme (case #1), results in uniform peak inter-story drifts and the least peak floor accelerations. The results illustrate that in the decentralized wireless control cases, the higher sampling rate (from lower communication latency) can potentially compensate for the lack of sensor data from faraway floors.

3. NUMERICAL SIMULATIONS INVESTIGATING THE PERFORMANCE OF DECENTRALIZED STRUCTURAL CONTROL

With the decentralized output feedback control algorithm validated through experiments, further analysis of decentralized control strategies is pursued via numerical simulations. A 20-story benchmark structure designed for the Structural Engineers Association of California (SAC) project is selected [13]. The structure represents a typical mid- to high-rise steel-frame building in the Los Angeles, Southern California region. To simplify the analysis, the building is modeled as an in-plane lumped-mass structure (Fig. 4). In the following, the decentralized control architecture for this 20-story building is first introduced. Then numerical simulation results for decentralized control are presented, assuming that the structure is instrumented with ideal actuators that are capable of producing any desired forces. This section includes simulation results for the case when the 20-story structure is installed with semi-active hydraulic dampers [14].

3.1 Decentralized control architecture

In the numerical simulations, it is assumed that both the inter-story displacements and inter-story velocities between every two neighboring floors are measurable. Similarly, the system state-space equations are formulated such that the state-space vector contains inter-story displacements and velocities, rather than the displacements and velocities relative to the ground. The output matrix $\mathbf{D_d}$ is defined as a $2n \times 2n$ identity matrix, so that the state-space vector is used for control feedback directly. The simulations are conducted for different degrees of centralization (DC), as illustrated in Fig. 4(c). The degrees of centralization reflect different wireless network architectures, with each wireless channel representing one wireless subnet. The actuators covered within a subnet are allowed to access the wireless sensor data within that subnet. For example, the case where DC=1 implies each wireless channel covers only five stories and a total of four wireless channels (subnets) are utilized. Of all the different degrees of centralization, the case where DC=1 represents the lowest requirement to the wireless communication range and achieves lowest communication latency as a

smaller number of wireless sensors need to broadcast their data in the subnet. Constrained by this decentralized information structure, the gain matrix for the case where DC=1 has the following sparsity pattern:

$$\mathbf{G_d} = \left[\begin{array}{cccc|cccc} \mathbf{G}^{(1,1)} & & & & \mathbf{G}^{(1,5)} & & & \\ & \mathbf{G}^{(2,2)} & & & & \mathbf{G}^{(2,6)} & & \\ & & \mathbf{G}^{(3,3)} & & & & \mathbf{G}^{(3,7)} & \\ & & & \mathbf{G}^{(4,4)} & & & & \mathbf{G}^{(4,8)} \end{array}\right]_{20\times 40}, \text{ when DC} = 1 \tag{8}$$

The left submatrix and the right submatrix correspond to the inter-story displacement and the inter-story velocity components, respectively, of the output vector $\mathbf{y_d}$. Each submatrix is block-diagonal, with every block $\mathbf{G}^{(i,j)}$ being a 5-by-5 square matrix.

For the case where DC=2, each wireless channel covers ten stories and a total of three wireless channels are utilized. Constrained by the overlapping information structure, the gain matrix for DC=2 has the following sparsity pattern:

$$\mathbf{G_d} = \left[\begin{array}{cccc|cccc} \mathbf{G}^{(1,1)} & \mathbf{G}^{(1,2)} & & & \mathbf{G}^{(1,5)} & \mathbf{G}^{(1,6)} & & \\ \mathbf{G}^{(2,1)} & \mathbf{G}^{(2,2)} & \mathbf{G}^{(2,3)} & & \mathbf{G}^{(2,5)} & \mathbf{G}^{(2,6)} & \mathbf{G}^{(2,7)} & \\ & \mathbf{G}^{(3,2)} & \mathbf{G}^{(3,3)} & \mathbf{G}^{(3,4)} & & \mathbf{G}^{(3,6)} & \mathbf{G}^{(3,7)} & \mathbf{G}^{(3,8)} \\ & & \mathbf{G}^{(4,3)} & \mathbf{G}^{(4,4)} & & & \mathbf{G}^{(4,7)} & \mathbf{G}^{(4,8)} \end{array}\right]_{20\times 40}, \text{ when DC} = 2 \tag{9}$$

For the case when DC=3, the number of stories covered by each wireless subnet increases accordingly. That leads to fewer communication subnets and fewer zero blocks in the gain matrices. The case where DC=4 specifies that one

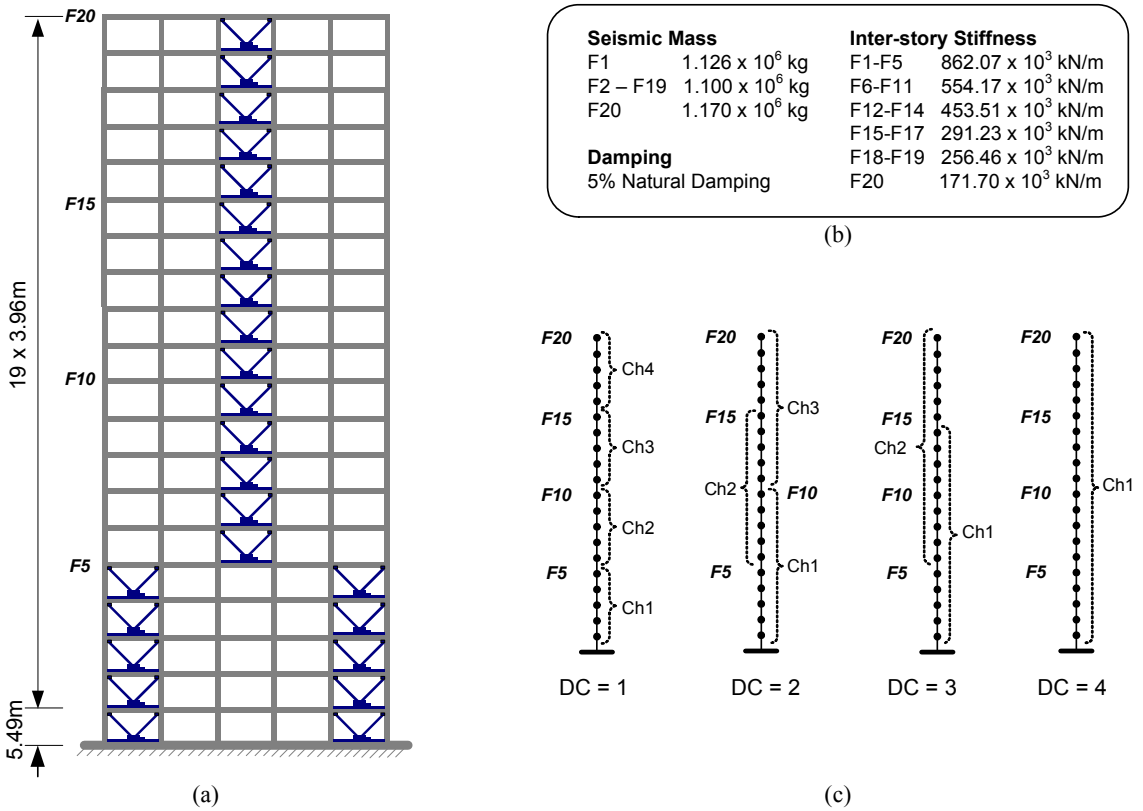

Fig. 4. Twenty-story SAC building [13] for numerical simulations: (a) building elevation; (b) model parameters of the lumped mass structure; (c) wireless subnet partitioning for different degrees of centralization (DC).

wireless channel covers all twenty floors, which results in a centralized information structure.

3.2 Numerical simulations using ideal actuators

To investigate the effectiveness of the decentralized control schemes proposed, we first assume the 20-story structure is instrumented with ideal actuators that produce any desired horizontal force between every two neighboring floors. Various combinations of centralization degrees (DC = 1,…,4) and sampling time steps ranging from 0.01s to 0.1s (at a resolution of 0.01s) are simulated. Additionally, three ground motion records are used for each simulation: the 1940 El Centro NS record (Imperial Valley Irrigation District Station), the 1995 Kobe NS record (JMA Station), and the 1999 Chi-Chi NS record (TCU-076 Station), all scaled to a peak ground acceleration (PGA) of 1m/s^2. Two representative performance indices proposed by Spencer *et al*. [13] are adopted:

$$PI_1 = \max_{\text{Earthquakes}} \left\{ \frac{\max\limits_{t,i} d_i(t)}{\max\limits_{t,i} \hat{d}_i(t)} \right\}, \text{ and } PI_2 = \max_{\text{Earthquakes}} \left\{ \frac{J_{LQR}}{\hat{J}_{LQR}} \right\} \tag{10}$$

Here PI_1 and PI_2 are the performance indices corresponding to inter-story drifts and LQR cost indices, respectively. In Eq. (10), $d_i(t)$ represents the inter-story drift between floor i (i = 1, …, n) and its lower floor at time t, and $\max\limits_{t,i} d_i(t)$ is the maximum inter-story drift over the entire time history and among all floors. The maximum inter-story drift is normalized by its counterpart $\max\limits_{t,i} \hat{d}_i(t)$, which is the maximum response of the uncontrolled structure. The largest normalized ratio among the simulations for the four different earthquake records is defined as the performance index PI_1. Similarly, the performance index PI_2 is defined for the LQR control index J_{LQR}, as given in Eq. (10). When computing the LQR index over time, a uniform time step of 0.001s is used to collect the structural response data points, regardless of the sampling time step of the control scheme; this allows one control strategy to be compared to another without concern for the different sampling time steps used in the control solution.

Values of the two control performance indices are plotted in Fig. 5 for different combinations of degrees of centralization and sampling time steps. The plots shown in Fig. 5(a) and 5(b) illustrate that the degrees of centralization and sampling steps have significant impact on the performance of the control system. Generally speaking, control performance is better for higher degrees of centralization and shorter sampling times. The plots show that except for the case where DC=1, the control schemes with certain overlapping information structures achieve comparable performance. To better review the simulation results, the performance indices for the four different control schemes are re-plotted as a function of sampling time in Fig. 5(c) and 5(d). As shown in Fig. 5(c), if a partially decentralized control system with DC equal to 2 can achieve a sampling step of 0.02s and a centralized system can only achieve 0.04s due to additional communication latency, the partially decentralized system can result in lower maximum inter-story drifts. Similar trends are observed in Fig. 5(d), except that the plots are smoother due to the summation process for computing the LQR indices.

3.3 Numerical simulations using semi-active hydraulic dampers

In general, structural actuators have certain capacity limits for actuation forces. Numerical simulations are conducted for decentralized control where semi-active hydraulic dampers (SHD) are employed on the structure. The arrangement of SHD dampers is shown in Fig. 6(a); the number of instrumented SHD dampers decreases gradually from 4 to 1 in the higher floors. If the desired damping force is in an opposite direction to the inter-story velocity, as shown in Fig. 6(b), the damping coefficient is adjusted so that a damper force closest to the desired force is generated. If the desired force is in the same direction to the inter-story velocity, the damping coefficient is set to its minimum value. Each SHD damper is installed as a V-brace underneath the corresponding floor. To accurately model the damping force, the Maxwell element proposed by Hatada *et al*. [14] is employed. In a Maxwell element, a dashpot and a stiffness spring are connected in series, which result in a damping force described by the following differential equation:

$$\dot{p}(t) + \frac{k_{eff}}{c_{SHD}(t)} p(t) = k_{eff} \Delta\dot{x}(t) \tag{11}$$

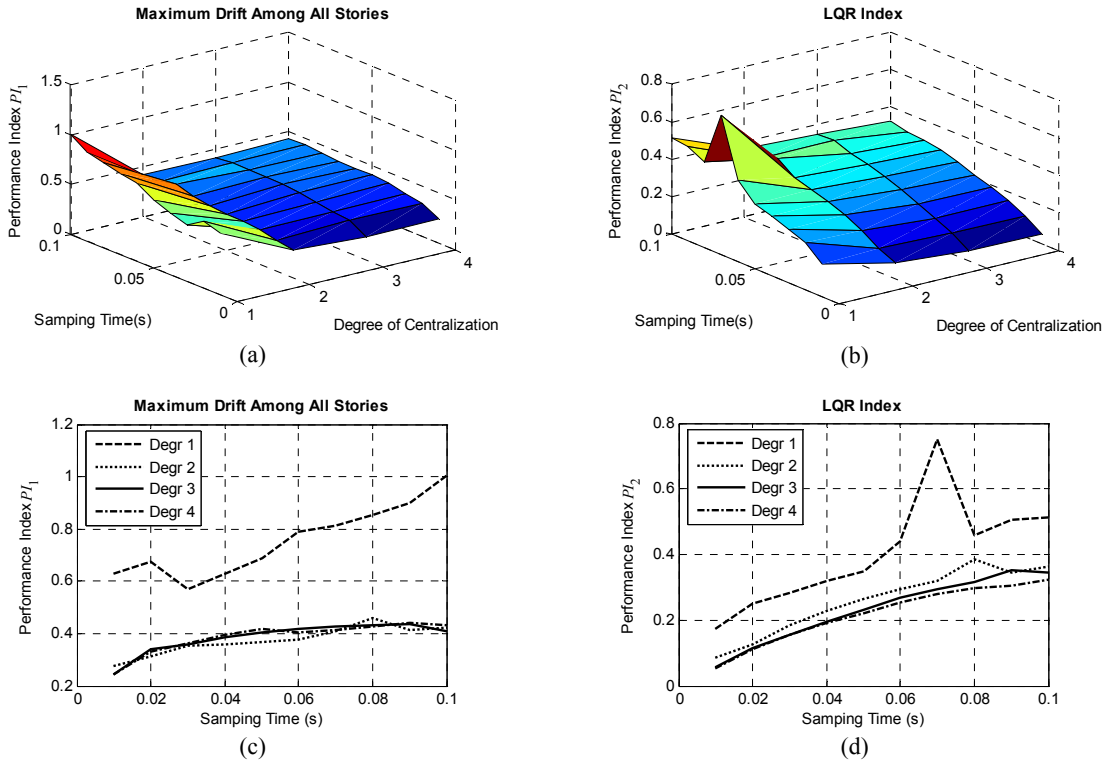

Fig. 5. Simulation results illustrating performance indexes for different sampling time steps and degrees of centralization (DC): (a) 3D plot for performance index PI_1; (b) 3D plot for performance index PI_2; (c) condensed 2D plot for PI_1; (d) condensed 2D plot for PI_2.

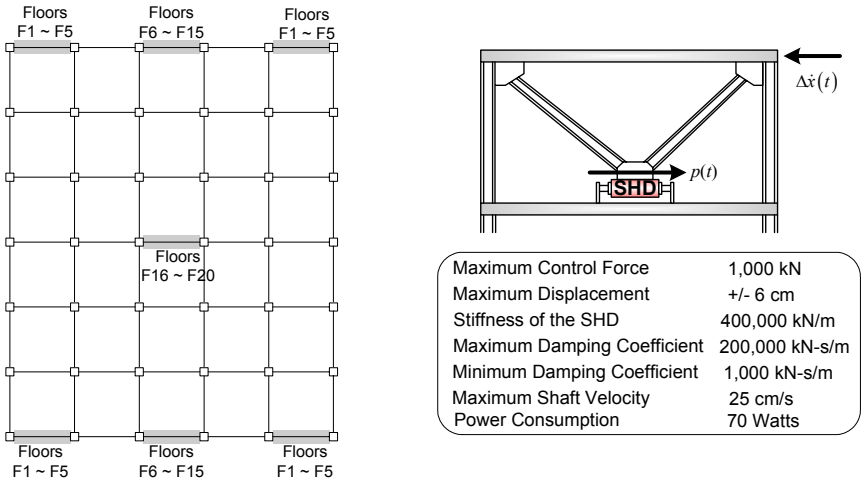

Fig. 6. Instrumentation of semi-active hydraulic dampers (SHD): (a) layout of SHD dampers on the floor plans; (b) key parameters of the SHD damper.

where $p(t)$ and $\Delta\dot{x}(t)$ denote the damping force and the inter-story velocity, respectively, k_{eff} represents the effective stiffness of the damper in series with the V-brace, and $c_{SHD}(t)$ is the adjustable damping coefficient of the SHD damper.

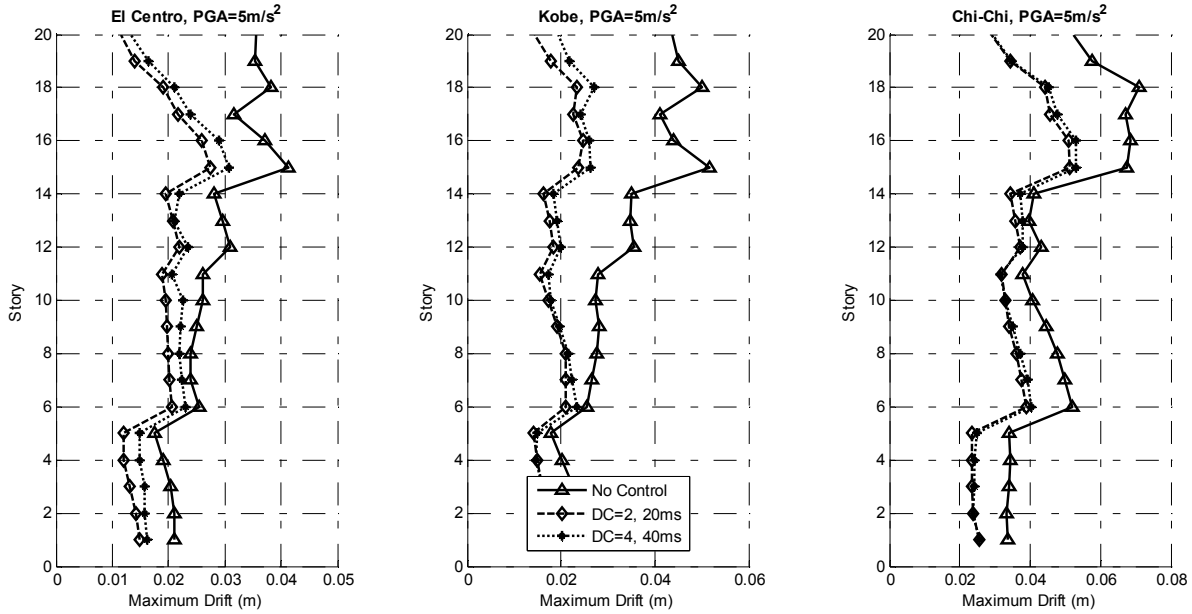

Fig. 7. Maximum inter-story drifts for cases where DC=2 with 20ms time delay and DC=4 with 40ms time delay.

Fig. 7 presents the simulated maximum inter-story drifts when the structure is excited using the same three ground motions as described in section 3.2, except that the PGAs are scaled up to $5m/s^2$, instead of $1m/s^2$. To compare the performance of decentralized versus centralized control, the case where DC=2 (partially decentralized) and the case where DC=4 (centralized) are plotted. As shown in Fig. 4, each wireless subnet covers ten floors when DC=2, or twenty floors when DC=4. That is, the induced time delay when DC=2 is about half of the delay when DC=4, and the time delays of 20ms and 40ms are assigned, respectively, for these two cases. As shown in Fig. 7, both of the two control schemes significantly reduce the maximum inter-story drifts compared with the uncontrolled case. For the Kobe and Chi-Chi ground motions, the partially decentralized case where DC=2 achieves equivalent performance compared with the centralized case where DC=4, while for the El Centro record, the case with DC=2 achieves slightly better performance than the case where DC=4. These results illustrate that although decentralized control has the disadvantage of computing control decisions without complete sensor data, the lower time delay in decentralized control could make the control scheme perform as well as centralized control, given that the centralized case requires longer communication latencies.

4. CONCLUSIONS

In this study, a prototype wireless structural sensing and control system is developed, and its performance validated in real-time feedback control experiments using a 3-story steel structure instrumented with MR dampers. Further simulation analyses are conducted using a 20-story building structure instrumented with ideal actuators and SHD dampers by varying the degrees of centralization and the sampling time steps of the control system. Both experimental and simulation results illustrate that decentralized control strategies may reduce system cost and provide equivalent or even superior control performance, given that their centralized counterparts could require longer sampling steps due to communication latencies in a wireless network.

5. ACKNOWLEDGMENTS

This research is partially funded by the National Science Foundation under grant CMS-0528867 and the Office of Naval Research Young Investigator Program awarded to Prof. Lynch at the University of Michigan. Additional support is provided by National Science Council in Taiwan under Grant No. NSC 94-2625-Z-002-031. The authors wish to thank

two graduate student fellowship programs: the Office of Technology Licensing Stanford Graduate Fellowship at Stanford University and the Rackham Grant and Fellowship Program at the University of Michigan. The authors would also like to express their gratitude to Dr. Pei-Yang Lin and Mr. Kung-Chun Lu at National Taiwan University, for their generous support for conducting the shake table experiments at NCREE, Taiwan.

REFERENCES

1. T. T. Soong and B. F. Spencer Jr., "Supplemental Energy Dissipation: State-of-the-art and State-of-the-practice," *Eng. Struct.* 24(3), 243-259, 2002.
2. S. Y. Chu, T. T. Soong, and A. M. Reinhorn, *Active, Hybrid and Semi-active Structural Control*, John Wiley & Sons Ltd., 2005.
3. E. G. Straser and A. S. Kiremidjian, *A Modular, Wireless Damage Monitoring System for Structures*, Report No. 128, John A. Blume Earthquake Eng. Ctr., Stanford University, Stanford, CA, USA, 1998.
4. J. P. Lynch and K. J. Loh, "A Summary Review of Wireless Sensors and Sensor Networks for Structural Health Monitoring," *Shock Vib. Dig.*, Sage Publications, 38(2), 91-128, 2005.
5. Y. Wang, A. Swartz, J. P. Lynch, K. H. Law, K.-C. Lu, and C.-H. Loh, "Wireless Feedback Structural Control with Embedded Computing," *Proc. of the SPIE 11th Intl. Symposium on Nondestructive Evaluation for Health Monitoring and Diagnostics*, San Diego, CA, USA, Feb 26 - Mar 2, 2006.
6. J. P. Lynch and D. Tilbury, "Implementation of a Decentralized Control Algorithm Embedded within a Wireless Active Sensor," *Proc. of the 2nd Annual ANCRiSST Workshop*, Gyeongju, Korea, Jul 21-24, 2005.
7. N. Sandell, Jr., P. Varaiya, M. Athans, and M. Safonov, "Survey of Decentralized Control Methods for Large Scale Systems", *IEEE Transactions on Automatic Control*, 23(2), 108-128, 1978.
8. Y. Wang, J. P. Lynch, and K. H. Law, "A Wireless Structural Health Monitoring System with Multithreaded Sensing Devices: Design and Validation," *Structure and Infrastructure Engineering - Maintenance, Management and Life-Cycle Design & Performance*, 3(2), 103-120, 2006.
9. L. L. Chung, C. C. Lin, and K. H. Lu, "Time-delay Control of Structures," *Earthquake Eng. Struct. Dyn.*, John Wiley & Sons, 24(5), 687-701, 1995.
10. J. Lunze, *Feedback Control of Large-scale Systems*, Prentice Hall, Hertfordshire, UK, 1992.
11. Y. Wang, R. A. Swartz, J. P. Lynch, K. H. Law, K.-C. Lu, and C.-H Loh, "Decentralized Civil Structural Control using a Real-time Wireless Sensing and Control System," *Proc. of the 4th World Conf. on Structural Control and Monitoring (4WCSCM)*, San Diego, CA, USA, Jul 11 - 13, 2006.
12. P.-Y. Lin, P. N. Roschke, and C.-H. Loh, "System Identification and Real Application of a Smart Magneto-Rheological Damper," *Proc. of the 2005 Intl. Symposium on Intelligent Control*, Limassol, Cyprus, Jun 27-29, 2005.
13. B. F. Spencer Jr., R. E. Christenson, and S. J. Dyke, "Next Generation of Benchmark Structural Control Problems for Seismically Excited Buildings." *Prof. of the 2nd World Conference on Structural Control*, Kyoto, Japan, Jun 28 - Jul 1, 1998.
14. T. Hatada, T. Kobori, M. Ishida, and N. Niwa, "Dynamic Analysis of Structures with Maxwell Model," *Earthquake Eng. Struct. Dyn.*, John Wiley & Sons, 29(2), 159-176, 2000.